Biochemical and Biophysical Research Communications 375 (2008) 405–409

Contents lists available at ScienceDirect

Biochemical and Biophysical Research Communications

journal homepage: www.elsevier.com/locate/ybbrc

Comparative models of P2X2 receptor support inter-subunit ATP-binding sites

Guillaume Guerlet [a], Antoine Taly [b], Lia Prado de Carvalho [a], Adeline Martz [a], Ruotian Jiang [a], Alexandre Specht [a], Nicolas Le Novère [c], Thomas Grutter [a,*]

[a] Department of Bioorganic Chemistry, UMR 7175 CNRS, Faculté de Pharmacie, Université Louis Pasteur, 67401 Illkirch, France
[b] UMR 7006, ISIS, Université Louis Pasteur, Strasbourg, France
[c] EMBL-EBI, Hinxton, EBI, Wellcome Trust Genome Campus, Hinxton, Cambridge, UK

ARTICLE INFO

Article history:
Received 1 August 2008
Available online 19 August 2008

Keywords:
Ligand-gated ion channel
P2X receptor
ATP
Purinergic
Gating
ASIC
Comparative modeling
Secondary structure predictions

ABSTRACT

ATP-gated P2X receptors (P2XRs) are ligand-gated ion channels (LGICs) presumably trimeric. To date, no experimental high-resolution structures are available. Recent X-ray structure of the acid-sensing ion channel 1 (ASIC1) revealed an unexpected trimeric ion channel. Beside their quaternary structure, P2XR and ASIC1 share common membrane topologies, but no significant sequence similarity. In order to overcome this low sequence resemblance, we have developed comparative models of $P2X_2R$ based on secondary structure predictions using the crystal structure of ASIC1 as template. These models were constrained to be consistent with known arrangement of disulfide bridges. They agreed with cross-linking experiments and supported inter-subunit ATP-binding sites. One of our models reconciled most existing data and provides new structural insights for a plausible mechanism of gating, thus encouraging new experiments.

P2X receptors (P2XR) are ligand-gated ion channels (LGICs). They are allosteric transmembrane proteins that convert ATP-binding into opening of an ion channel [1]. The channel is probably homo- or heterotrimeric [2]. Each subunit ($P2X_{1-7}$) possesses intracellular amino and carboxyl termini and two transmembrane segments (TM1 and TM2), joined by an extracellular ectodomain containing 10 highly conserved cysteine residues presumably engaged in disulfide bridges [3,4] (Fig. 1). Unlike other LGICs [5], no crystal structure has been resolved for P2XR.

The absence of sequence similarity to known crystallized proteins reduces the possibilities to produce homology-based models, and information about the molecular structure of these receptors has been essentially indirect [6]. These studies identified residues K69, K71, F183, K188, F289, R290, and K308 (rat $P2X_2$ numbering) as involved in modulation of P2X function by ATP. So far only partial models of the ATP-binding site have been proposed [6,7].

The X-ray structure of acid-sensing ion channel subtype 1 (ASIC1), a member of the degenerin and epithelial sodium channel family, was recently determined at 1.9 Å resolution and reveals an unexpected trimeric ion channel [8] (Fig. 1B). Beside the trimeric structure, P2XR and ASIC1 also display a central pore lined primarily by TM2 residues [8,9], and share a common membrane topology (Fig. 1C). Both present a highly conserved cysteine-rich domain although arranged differently (Fig. 1).

Here, we propose that P2XR and ASIC1 share a similar three-dimensional scaffold. We present three different comparative models of $P2X_2R$ based on secondary structure predictions using the crystal structure of ASIC1 as template. These models were analyzed in the light of experimental data and support an inter-subunit ATP-binding site. The third model reconciles almost all available experimental data, providing the first plausible molecular model of a complete P2XR.

Methods

Twenty three homologous mammalian sequences of $P2X_{1-6}Rs$ were extracted from UniProtKB (listed in Supplementary Fig. 1). The sequences were aligned with ClustalX [10]—using default parameters—in order to eliminate those presenting large insertions or deletions, and to align subsequent structure predictions. The membrane topology of the P2X receptor subunit sequences was predicted using two independent approaches. TopCons (http://topcons.net/), is a consensus prediction tool using first principles, such as SCAMPI and ΔG-scale, and supervised learning methods such as OCTOPUS, ZPRED and PRODIV-TMHMM. MEMSAT3 is a cascading neural network [11]. Those methods predict the location of transmembrane domains but also their orientation. The secondary structure of each sequence was predicted using PSI-PRED, a

* Corresponding author. Fax: +33 3 90 24 43 06.
E-mail address: grutter@bioorga.u-strasbg.fr (T. Grutter).

0006-291X/$ - see front matter © 2008 Elsevier Inc. All rights reserved.
doi:10.1016/j.bbrc.2008.08.030

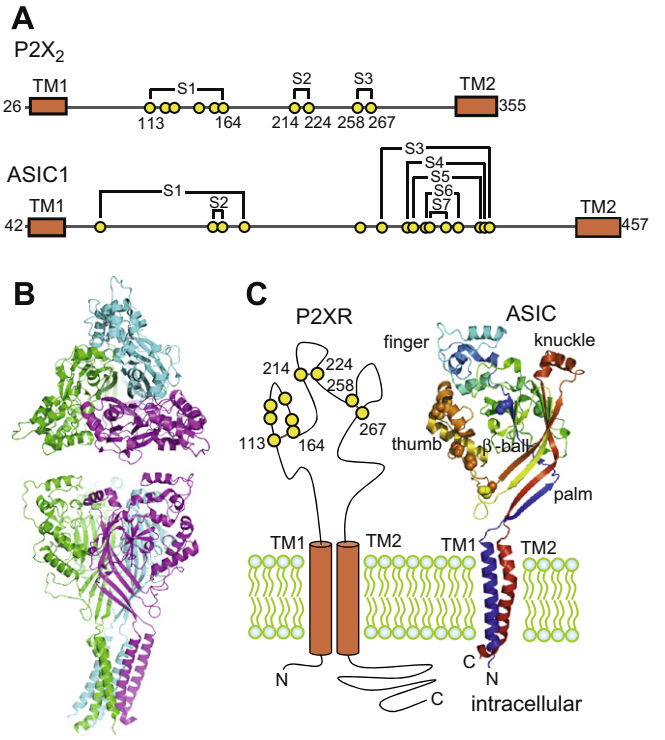

Fig. 1. (A) Schematic representation of a $P2X_2$ and ASIC1 subunit. Conserved cysteine residues (yellow spheres) linked through disulfide bridges (S1 to S7) are indicated. (B) Top and lateral views of ASIC1 crystal structure. (C) Membrane topology predicted for $P2X_2$ and experimentally determined for ASIC1 (one monomer shown).

cascading neural network coupled with position-specific matrices [12]. The different predictions generated consensus transmembrane topology and secondary structure predictions for $P2X_2$. Alignments between the sequences of rat $P2X_2$ and chicken ASIC1 were performed using $P2X_2$ structure predictions and ASIC1 experimental structure (PDB entry 2QTS). These alignments were used to build comparative models of $P2X_2$ with the program MODELLER8v2 [13]. In the aligned regions, the program uses ASIC1 (trimer ABC [8]) as a template to build a tentative backbone for $P2X_2$. The portions of $P2X_2$ without equivalent in ASIC1 are built *ab-initio* by MODELLER. The software then solves the structure problems by satisfying spatial constraints, including disulfide bonds if specified. In model 1, residues V87 to T112 corresponding to *ab-initio* construct were omitted enabling C113 to be linked to C164. Structure quality assessment was performed with Procheck (http://www-nmr.cabm.rutgers.edu/PSVS/). The accuracy per chain was determined by: $Q3 = p_{\text{alpha}} + p_{\text{beta}} + p_{\text{coil}}/\text{lenght}$, where p_i is the number of correctly predicted residues in the state *i*.

Results

General strategy for the alignment between $P2X_2$ and ASIC1

Multiple sequence alignment of $P2X_{1-6}$ identified highly conserved regions (Supplementary Fig. 1). The predicted membrane topology of P2XRs suggested two transmembrane segments joined by the large extracellular domain as previously determined [14]. Secondary structure predictions revealed alternation between α-helices and β-strands, with an excess of the latter (Supplementary Fig. 2B). Comparison of the predicted secondary structures of ASIC1 with the X-ray structure revealed a very close matching between prediction and experiment (Q3: 83.82%; Supplementary Fig. 2A), confirming the high level of prediction confidence.

The sequence of ASIC1 ectodomain was found to be longer than that of $P2X_2$ (by around 100 residues) and the X-ray structure revealed more α-helices for ASIC1 than those predicted for $P2X_2$ (Supplementary Fig. 2B). ASIC1 α-helices were folded in substructures, the finger (α1 to α3), the thumb (α4 to α5), and the knuckle (α6 to α7), in which the N- and C-terminal residues of each subdomain were very close (Supplementary Fig. 3C). These helices were located on the external face of the protein, outside of the internal palm and β-ball (Fig. 1C). As predictions for P2XR showed less α-helices, we chose to ignore one (or more) of these subdomains, with the assumption that its (their) absence should not perturb the general folding of the protein.

Cysteine residues of $P2X_2$ and ASIC1 do not align well. Thus, we used the arrangement of disulfide bonds experimentally determined for P2XR (S1:C113/C164, S2:C214/C224, and S3:C258/C267) [3,4]. Based on the crystal structure of ASIC1, we paired these cysteines imposing strong geometrical constrains.

Building the models and experimental validation

Initial model and its refinement

The secondary structure prediction of $P2X_2$ was aligned to that experimentally determined for ASIC1, anchoring on the two transmembrane domains. This initial alignment, ignoring the thumb in ASIC1, revealed a close assignment in regions following TM1 and preceding TM2 (Supplementary Fig. 2B). However, differences were observed at the level of the finger and knuckle (Supplementary Fig. 2B). The alignment was then used to build an initial comparative model, which was challenged with existing data.

First, residues V48 and I328, two residues previously suggested to be close at the subunit interface [15], were located on two adjacent α-helices between subunits at a short distance from each other (<11 Å from their Cα atoms). However, side chain of I328 did not face directly that of V48, but was rotated by ~100° (Supplementary Fig. 2C). Second, residues shown to participate to the ion-conducting pathway (I332, T336, T339, and V343), were on the same side of the helix, but away from the lumen of the ion channel, again rotated by ~100° (Supplementary Fig. 2C). Third, K69 was located far from F289 (~36 Å; Supplementary Fig. 2D), inconsistent with the close proximity of these residues as determined by cross-linking [16]. Last, residues K69, K71, and K308 were proximal, but their side chains pointed outward (not shown), also inconsistent with the idea that these residues participate to the ATP-binding site.

We thus refined the alignment by (i) ignoring the knuckle, (ii) slightly shifting the alignment in regions close to TMs, and (iii) shifting the alignment by one position in TM2 (100° rotation in the α-helix). We then produced three different alignments and their alternatives (these last corresponded to the elimination of the gap before TM2 in ASIC1; Supplementary Fig. 3).

Model 1

Alignment 1 was better than initial alignment in region β1–β2 and prior to TM2 (Supplementary Fig. 3A). The corresponding model 1 showed a better Ramachandran plot than the initial model (Supplementary Table 1). The first loop (C113/C164), corresponding to the finger in ASIC1, was folded in a globular domain, in which C124 was close to C158 (Fig. 2A). The two other loops (C214/C224 and C258/C267) did not align to ASIC1 and were modeled *ab-initio*. The three residues N182, N239, and N298, previously shown to be glycosylated in $P2X_2R$ [14,17], were outside the protein (not shown).

As expected, side chains of both V48 and I328 faced each other at the subunit interface (average distance of Cα atoms for three subunits: 8.6 Å), and those of K69, K71, and K308 pointed towards

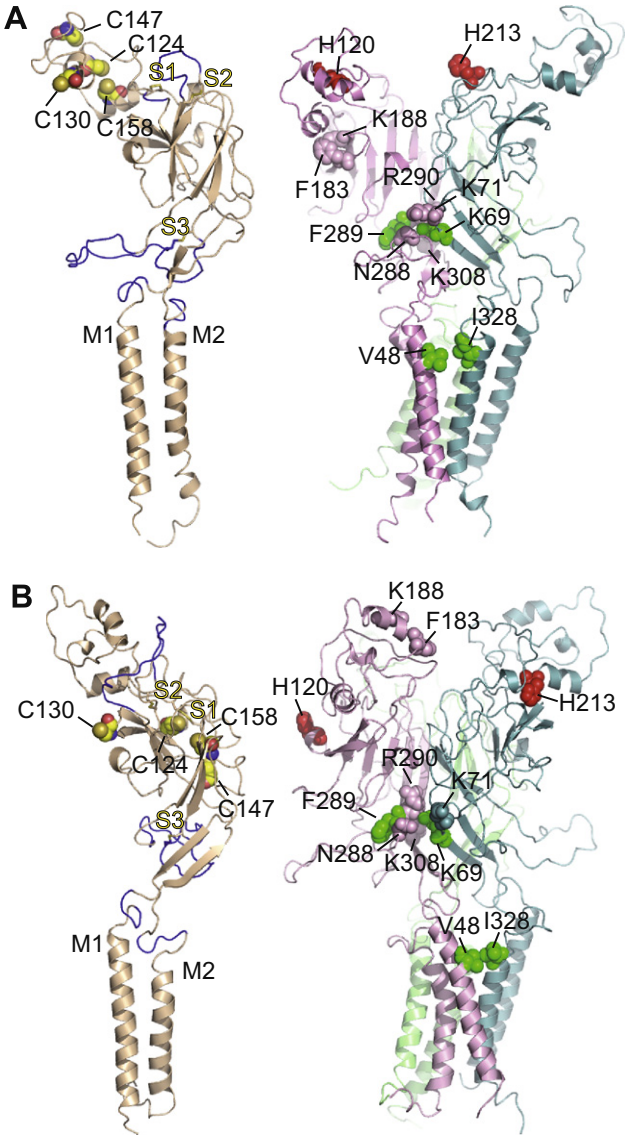

Fig. 2. Comparative models 1 (A) and 2 (B) of $P2X_2R$. *Left*, *Ab-initio* constructions are highlighted in blue (one monomer shown). Disulfide bonds (stick) and conserved cysteine residues (spheres) are indicated. *Right*, Residues that fit (green spheres), or not (red), with previous disulfide cross-linking data are highlighted (trimer shown). Also indicated residues previously suggested to participate into the putative ATP-binding site. Subunits are differentially colored.

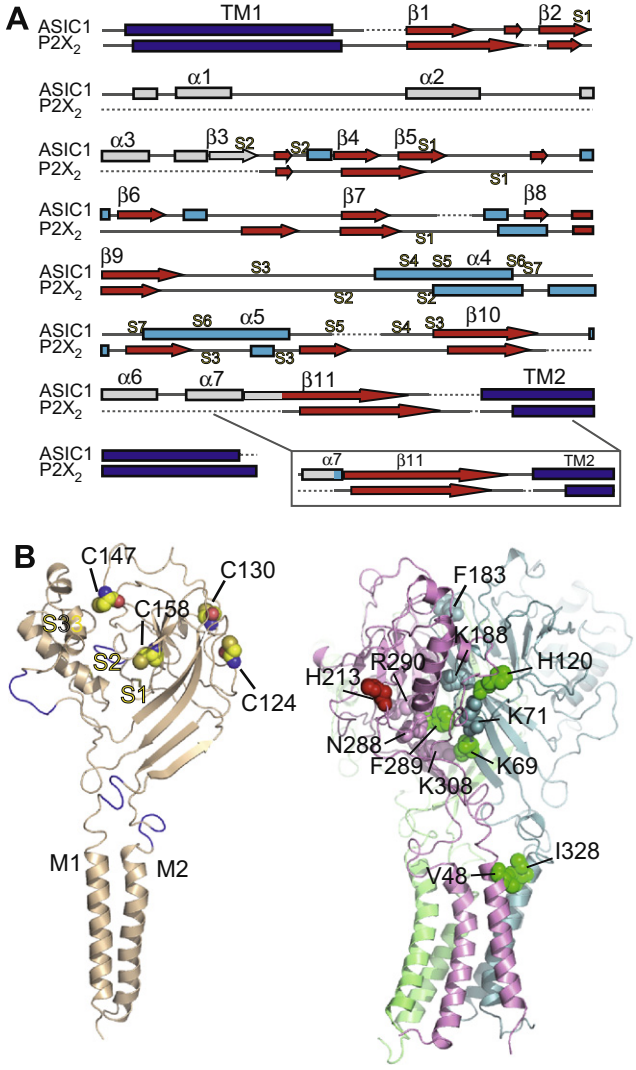

Fig. 3. (A) Alignment 3 secondary structure between ASIC1 (experimentally determined) and $P2X_2$ (predicted). Also shown the disulfide connectivity. Structures in ASIC1 that were ignored for modeling are colored grey. Inset: alternative alignment 3B. (B) Corresponding comparative model 3 of $P2X_2R$. Same representation as in Fig. 2

a possible interfacial pocket (Fig. 2A). In the alternative comparative model 1B, K308 was located outside this pocket (not shown). Interestingly, ignoring the knuckle re-located residue F289 very close to K69 (11.3 Å), although their side chains did not face each other, but most importantly, these two residues were at the subunit interface (Fig. 2A), a finding that is consistent with cross-linking data [16].

Even though model 1 agreed well with experimental data, several weaknesses were observed. First, F183 and K188, two additional residues proposed to participate in ATP-binding [18,19], were far from K69 and F289 (Fig. 2A). Second, H120 and H213, two residues previously shown to form the allosteric Zn^{2+}-binding site at the subunit interface in $P2X_2R$ [20], were too far apart to coordinate Zn^{2+} (33.4 Å; Fig. 2A). Third, different secondary structure assignments were still observed at the level of the finger (helix α3, Supplementary Fig. 3A).

Model 2

The region 113 to 164 of $P2X_2$ was predicted in β-strands whereas α-helices are observed in the corresponding region of ASIC1, 97 to 164. Conversely, the region 165–225 of ASIC1 shows more β-strands structure than the corresponding region in $P2X_2$, predicted both in α-helix and β-strand (Supplementary Fig. 3A and 3B). Furthermore, the connecting residues 97, 165, and 226 are very close to each other in ASIC1 allowing formation of the peptide bond between 97 and 165, 226 and 98, and 164 and 227 (Supplementary Fig. 3C). Therefore, to improve model 1, we generated alignment 2 containing a circular permutation of positions 97–164 and 165–225 of ASIC1 (Supplementary Fig. 3B). Such circular permutation was already observed in saposin domains, appropriately named 'swaposins' [21].

The resulting model 2 also displayed a satisfactory Ramachandran plot (Supplementary Table 1). The three conserved cysteines C124, C147, and C158 were close to each other (11–13 Å), however C130 was far from these residues (Fig. 2B). Furthermore, the three *N*-glycosylation sites were outside of the protein (not shown). As the circular permutation did not involve residues V48, K69, F289,

and I328, model 2 (and its alternative model 2B) also agreed with the cross-linking data (Fig. 2B). On the other hand, H120 and H213 were too far to fit with a possible interfacial Zn^{2+}-binding site and F183 and K188 were not close to the putative ATP-binding site (Fig. 2B). Thus, the circular permutation did not improve the model.

Model 3

Alignment 3, reintroducing the thumb of ASIC1, but ignoring the finger and strand β3, displayed no strong divergences of secondary structure assignments (Fig. 3A). Almost all of the $P2X_2$ sequence was successfully aligned to ASIC1, providing a full-modeled structure thus limiting considerably *ab-initio* construction (Fig. 3).

Model 3 revealed a more compact structure with satisfying Ramachandran plot (Supplementary Table 1). The first loop (C113/C164) was folded partially in the corresponding β-ball structure while the two others (C214/C224 and C258/C267) were modeled in the corresponding thumb (Fig. 3B). In the first loop, C130 was close to C124 (~10 Å) and C147 was 16 Å away from C158. In addition, residues N182, N239, and N298, were on the external face of the protein (not shown). As expected, the location and distance between K69 and F289 (10.9 Å), and V48 and I328 (8.5 Å, Fig. 3B) were similar, as in models 1 and 2 (and alternatives B) since the alignment for these positions did not change, except one position shift in β10 enabling side chain of F289 to point towards K69.

Interestingly H120, involved in coordinating Zn^{2+} ion [20], was at the subunit interface (Fig. 3B). However, H213 was too distant from H120 (~24 Å) to form a coordinating-binding site (Fig. 3B). In addition, residue K188, important in ATP function [7,19], was close to the putative ATP-binding site, although its neighboring residue F183 was not (Fig. 3B). Finally, a last outcome of this model is that H120 was close to residue K69 (~15 Å appart), thus positioning V119 (homologous to R125 in $P2X_7R$) close to the putative ATP-binding site (Fig. 4A), as proposed recently in $P2X_7R$ [22]. Overall, model 3 best matched existing experimental data.

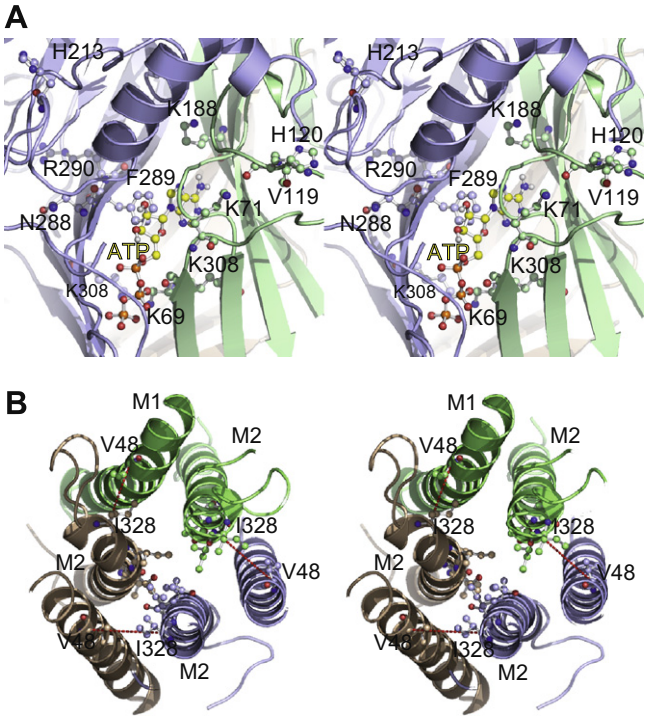

Fig. 4. (A) Stereo view of the putative ATP-binding site of model 3. Putative ATP-binding residues are indicated. Also shown ATP and residues V119, H120, and H213. For clarity, backbone corresponding to residues 272–284 is omitted. (B) Stereo view from the extracellular side, along the pore axis, of the ion channel of model 3. Residues in TM2 previously shown to be accessible to thiol-specific reagents (I332, T336, T339, and V343) are located in the lumen of the ion channel. Also indicated V48 and I328 and the distance separating their Cα atoms (red dotted lines). Subunits are differentially colored.

Discussion

We propose that P2XR and ASIC1 are similarly folded despite the absence of significant sequence similarity. We produced three comparative models of the complete $P2X_2R$ (without the intracellular loops) that agree with existing cross-linking experiments, with an expected water-accessible position of glycosylation sites and with a possible interfacial ATP-binding site. The third model (Fig. 3) best matched several criteria and further reconciled additional experimental data: (i) the best score for the alignment, (ii) a more compact structure, (iii) the possible location of K188 to the putative ATP-binding site, (iv) a possible interfacial location of the Zn^{2+}-binding residue H120, and (v) a close proximity of the ADP-ribosylation site to the putative ATP-binding site.

The ATP-binding site

In model 3, residues K69, K71, K188, N288, F289, R290, K308, previously suggested to take part in ATP-binding [6,7], line a possible pocket of 12–19 Å edges, comparable with the size of ATP (Fig. 4A). Docking of ATP was not performed. However, an extended conformation of ATP was manually placed at the subunit interface, illustrating the fact that its size is compatible with a plausible pocket lined by these residues.

Our models show an inter-subunit location of the putative ATP-binding site, as recently suggested by cross-linking experiments [16]. In Model 3, K69 and F289 from the neighboring subunit are separated by ~11 Å, a distance compatible with backbone motions (from 4.5 to 15.2 Å) determined through disulfide cross-linking [23]. Model 3 suggests that K69 is close to K308 at the subunit interface (Fig. 4A), as recently suggested [24]. However, in alternative model 3B, K308 was not in the putative ATP-binding site (not shown), also consistent with the fact that this residue might be important for gating [25]. Thus, we cannot yet exclude the alternative model 3B. Overall, these findings suggest that model 3 (and its alternative model 3B) represents a plausible model of the ATP-binding site.

An interesting outcome of model 3 is the close proximity of V119 to the putative ATP-binding site (Fig. 4A). A recent study has suggested that R125 in $P2X_7R$, homologous to V119, is close to the ATP-binding site, on the basis that ADP-ribosylation at this position gates the $P2X_7$ ion channel [22]. The distance separating V119 from the putative ATP-binding site is ~15 Å, a distance compatible with the length of the ADP-ribose. Model 3 thus offers a plausible structural illustration for the hypothesis [22] that the chemical framework of the adenine-ribonucleotide moiety fits into the nucleotide-binding site in $P2X_7R$.

The ion channel and a plausible molecular mechanism of gating for P2X

The three models show, as exemplified in model 3 (Fig. 4B), an expected M2 lumen location of I332, T336, T339, and V343, recently shown to participate in the ion-conducting pathway [9]. In addition, residues V48 and I328 are in close apposition (8.5 Å) at the subunit interface (Fig. 4B), in agreement with cross-linking engineering [15]. Note, however, that these residues are not symmetrically arranged around the axis due to the use as template of

the trimeric structure of ASIC1, which displays strong asymmetry in the ion channel. This asymmetry could be inherent to the crystal lattice contacts [8]. Thus, it is difficult to assign precisely which amino acids constitute the gate.

A structural outcome of model 3 is the presence of the thumb, proposed to be critical in ASIC1 gating [8]. The thumb covers partially the putative ATP-binding site and carries H213, one of the two residues involved in the allosteric Zn^{2+} modulation. An attractive hypothesis is that gating of the P2XR is similar to that previously proposed for ASIC1 [8]: the binding of ATP would change the conformation of the thumb, which subsequently would open the ion channel through interactions with the two TM α-helices. If this mechanism is correct, then the thumb would have a role similar to the "cys-loop" in the pentameric LGICs, where this loop interacts with residues connecting TM2 and TM3 [26].

Limitations of the models

Model 3 best reconciles most of the experimental data, but still shows weaknesses: (i) F183 was not positioned in the putative ATP-binding site; however, a recent study shows that this residue might not be in the ATP-binding site [27]; (ii) residues C124, C130, C147, and C158 are not engaged in disulfide bonds as previously suggested [3], even though some are sufficiently close to each other to be linked; however as precise assignment of these disulfide pairs still remains elusive [4], we chose not to impose this geometrical constrain; (iii) there is a different secondary structure assignment at the beginning of α5 (part of a the thumb). The low quality of the model in that region is also seen at the level of the intra-helix C258/C267 disulfide bond, and (iv) H213, also located in the thumb, was not close to H120, inconsistent with a correct coordination of Zn^{2+} necessary for potentiation of ATP responses in $P2X_2R$ [20] (Fig. 4A). However, this might be explained by the fact that the receptor may be in a closed state since the ASIC1 structure template was suggested to be in a closed, desensitized-like state [8]. Thus, opening the pore may produce conformational changes that bring H213 close to H120. For all these reasons, our models, although encouraging and stimulating new experiments, should *not* be taken as definitive.

In conclusion, we present three different comparative models of the complete $P2X_2R$ (except the intracellular loops). Model 3 best reconciles most of the experimental data and is in agreement with the compact structure of $P2X_4R$, recently determined at low resolution by electron microscopy [28]. Our results suggest that despite the absence of sequence resemblance, the three-dimensional folding of P2XR might be similar to that of ASIC1 and consequently the gating mechanisms might share some common features. Future experiments will challenge this hypothesis.

Acknowledgments

Work supported by ANR (06-0050-01) and CNRS. A.T. was a fellow from FRM. Authors are grateful to Prof. M. Goeldner.

Appendix A. Supplementary data

Supplementary data associated with this article can be found, in the online version, at doi:10.1016/j.bbrc.2008.08.030.

References

[1] B.S. Khakh, R.A. North, P2X receptors as cell-surface ATP sensors in health and disease, Nature 442 (2006) 527–532.
[2] N.P. Barrera, S.J. Ormond, R.M. Henderson, R.D. Murrell-Lagnado, J.M. Edwardson, Atomic force microscopy imaging demonstrates that $P2X_2$ receptors are trimers but that $P2X_6$ receptor subunits do not oligomerize, J. Biol. Chem. 280 (2005) 10759–10765.
[3] S.J. Ennion, R.J. Evans, Conserved cysteine residues in the extracellular loop of the human $P2X_1$ receptor form disulfide bonds and are involved in receptor trafficking to the cell surface, Mol. Pharmacol. 61 (2002) 303–311.
[4] J.D. Clyne, L.F. Wang, R.I. Hume, Mutational analysis of the conserved cysteines of the rat $P2X_2$ purinoceptor, J. Neurosci. 22 (2002) 3873–3880.
[5] R.J. Hilf, R. Dutzler, X-ray structure of a prokaryotic pentameric ligand-gated ion channel, Nature 452 (2008) 375–379.
[6] R.J. Evans, Orthosteric and allosteric binding sites of P2X receptors, Eur. Biophys. J. (2008).
[7] Z. Yan, Z. Liang, T. Obsil, S.S. Stojilkovic, Participation of the K313-I333 sequence of the purinergic $P2X_4$ receptor in agonist binding and transduction of signals to the channel gate, J. Biol. Chem. 281 (2006) 32649–32659.
[8] J. Jasti, H. Furukawa, E.B. Gonzales, E. Gouaux, Structure of acid-sensing ion channel 1 at 1.9 Å resolution and low pH, Nature 449 (2007) 316–323.
[9] M. Li, T.H. Chang, S.D. Silberberg, K.J. Swartz, Gating the pore of P2X receptor channels, Nat. Neurosci. (2008).
[10] J.D. Thompson, T.J. Gibson, F. Plewniak, F. Jeanmougin, D.G. Higgins, The CLUSTAL_X windows interface: flexible strategies for multiple sequence alignment aided by quality analysis tools, Nucleic Acids Res. 25 (1997) 4876–4882.
[11] D.T. Jones, Improving the accuracy of transmembrane protein topology prediction using evolutionary information, Bioinformatics 23 (2007) 538–544.
[12] D.T. Jones, Protein secondary structure prediction based on position-specific scoring matrices, J. Mol. Biol. 292 (1999) 195–202.
[13] A. Sali, T.L. Blundell, Comparative protein modelling by satisfaction of spatial restraints, J. Mol. Biol. 234 (1993) 779–815.
[14] A. Newbolt, R. Stoop, C. Virginio, A. Surprenant, R.A. North, G. Buell, F. Rassendren, Membrane topology of an ATP-gated ion channel (P2X receptor), J. Biol. Chem. 273 (1998) 15177–15182.
[15] L.H. Jiang, M. Kim, V. Spelta, X. Bo, A. Surprenant, R.A. North, Subunit arrangement in P2X receptors, J. Neurosci. 23 (2003) 8903–8910.
[16] B. Marquez-Klaka, J. Rettinger, Y. Bhargava, T. Eisele, A. Nicke, Identification of an intersubunit cross-link between substituted cysteine residues located in the putative ATP binding site of the $P2X_1$ receptor, J. Neurosci. 27 (2007) 1456–1466.
[17] G.E. Torres, T.M. Egan, M.M. Voigt, N-Linked glycosylation is essential for the functional expression of the recombinant $P2X_2$ receptor, Biochemistry 37 (1998) 14845–14851.
[18] J.A. Roberts, R.J. Evans, ATP binding at human $P2X_1$ receptors. Contribution of aromatic and basic amino acids revealed using mutagenesis and partial agonists, J. Biol. Chem. 279 (2004) 9043–9055.
[19] Z. Yan, Z. Liang, M. Tomic, T. Obsil, S.S. Stojilkovic, Molecular determinants of the agonist binding domain of a P2X receptor channel, Mol. Pharmacol. 67 (2005) 1078–1088.
[20] N. Nagaya, R.K. Tittle, N. Saar, S.S. Dellal, R.I. Hume, An intersubunit zinc binding site in rat P2X2 receptors, J. Biol. Chem. 280 (2005) 25982–25993.
[21] C.P. Ponting, R.B. Russell, Swaposins: circular permutations within genes encoding saposin homologues, Trends Biochem. Sci. 20 (1995) 179–180.
[22] S. Adriouch, P. Bannas, N. Schwarz, R. Fliegert, A.H. Guse, M. Seman, F. Haag, F. Koch-Nolte, ADP-ribosylation at R125 gates the $P2X_7$ ion channel by presenting a covalent ligand to its nucleotide binding site, FASEB J. 22 (2008) 861–869.
[23] C.L. Careaga, J.J. Falke, Thermal motions of surface alpha-helices in the D-galactose chemosensory receptor. Detection by disulfide trapping, J. Mol. Biol. 226 (1992) 1219–1235.
[24] W.J. Wilkinson, L.H. Jiang, A. Surprenant, R.A. North, Role of ectodomain lysines in the subunits of the heteromeric P2X2/3 receptor, Mol. Pharmacol. 70 (2006) 1159–1163.
[25] L. Cao, M.T. Young, H.E. Broomhead, S.J. Fountain, R.A. North, T339-to-serine substitution in rat P2X2 receptor second transmembrane domain causes constitutive opening and indicates a gating role for K308, J. Neurosci. 27 (2007) 12916–12923.
[26] T. Grutter, L. Prado de Carvalho, V. Dufresne, A. Taly, S.J. Edelstein, J.P. Changeux, Molecular tuning of fast gating in pentameric ligand-gated ion channels, Proc. Natl. Acad. Sci. USA 102 (2005) 18207–18212.
[27] J.A. Roberts, H.R. Digby, M. Kara, S.E. Ajouz, M.J. Sutcliffe, R.J. Evans, Cysteine substitution mutagenesis and the effects of methanethiosulfonate reagents at P2X2 and P2X4 receptors support a core common mode of ATP action at P2X receptors, J. Biol. Chem. 283 (2008) 20126–20136.
[28] M.T. Young, J.A. Fisher, S.J. Fountain, R.C. Ford, R.A. North, B.S. Khakh, Molecular shape, architecture and size of $P2X_4$ receptors determined using fluorescence resonance energy transfer and electron microscopy, J. Biol. Chem., in press.